

NiSe₂-CoSe₂ with a Hybrid Nanorods and Nanoparticles Structure for Efficient Oxygen Evolution Reaction

Meng Li¹ and Ligang Feng^{1*}

¹School of Chemistry and Chemical Engineering, Yangzhou University, Yangzhou 225002, China

Corresponding authors. Email: ligang.feng@yzu.edu.cn; fenglg11@gmail.com (L Feng*)

EXPERIMENT SECTION

1. Materials

All chemicals were of analytical grade and used without further purification. Nickel nitrate hexahydrate [Ni(NO₃)₂·6H₂O], cobalt nitrate hexahydrate [Co(NO₃)₂·6H₂O], ammonium fluoride (NH₄F), selenium powder, urea, ethylene glycol, and potassium hydroxide (KOH) were obtained from Aladdin Bio-Chem Technology Ni. LTD. (Shanghai, China). The commercial IrO₂ was obtained from Shanghai Macklin Biochemical Co., Ltd. Nafion (5 wt%) and ethanol were purchased from Sigma-Aldrich. Deionized water was purified using a water purification system with a resistance of 18.2 MΩ (Thermo Fisher Scientific Ni. LTD, USA).

2. Catalysts Fabrication

Synthesis of NiCo(OH)_x Precursor. For the synthesis of NiCo(OH)_x precursor, 2 mmol Ni(NO₃)₂·6H₂O and 2 mmol Co(NO₃)₂·6H₂O were dissolved in 60 mL ethylene glycol, and then 4 mmol urea and 3 mmol NH₄F were added into the solution forming a homogeneous solution with continuous stirring for 20 min. Afterward, the mixture was transferred into a Teflon-lined stainless steel autoclave and maintained at 120 °C for 6 hours. After the autoclave was cooled down to room temperature, the cyan powder was washed by ethanol and deionized water several times. Finally, the product was dried in a vacuum oven at 60 °C for overnight and denoted as NiCo(OH)_x precursor.

Synthesis of NiSe₂-CoSe₂. For the synthesis of NiSe₂-CoSe₂, the above prepared NiCo(OH)_x precursor of 100 mg was placed on an alumina boat and located on the downstream side; the other boat containing 600 mg selenium powders was put on the upstream side. N₂ gas with a flow rate of 100 sccm was used as the carrier gas. The furnace was heated by a heat ramp of 2 °C min⁻¹ and maintained at 350 °C for 3 hours, and then cooled down to room temperature. The obtained product was named as NiSe₂-CoSe₂.

Synthesis of NiSe₂ and CoSe₂. NiSe₂ and CoSe₂ were synthesized based on our previous work.^[1] In brief, Ni(OH)_x and Co(OH)_x precursors were synthesized through a facile and scalable solvothermal-assisted synthesis method. Then, the above prepared Ni(OH)_x/Co(OH)_x nanosheet of 50 mg was put face down on an alumina boat and located on the downstream side; the other boat containing 400 mg selenium powders was put on the upstream side. N₂ gas with a flow rate of 100 sccm was used as the carrier gas. The furnace was heated by a heat ramp of 2 °C·min⁻¹ and maintained at 350 °C for 3 hours, and then cooled down to room temperature. The obtained product was named NiSe₂/CoSe₂.

3. Physical Characterizations

The crystal structures of products were conducted by Powder X-ray diffraction (XRD, Bruker D8 X-ray diffractometer) using a Cu K_α (λ = 1.5405 Å) radiation source operating at 40 kV and 40 mA at a scanning rate of 5 °C·min⁻¹. The surface analysis of samples was examined by X-ray photoelectron spectroscopy (XPS, ECSALAB 250Xi, Al K_α radiation). The micro-morphologies of as-prepared catalysts were observed through scanning electron microscopy (SEM, FEI Sirion-200). The transmission electron microscopy and High-resolution transmission electron microscopy (HRTEM) were performed on an FEI Tecnai G2 F30 STWIN (USA) operating at 300 kV. X-ray detector spectrum (EDS) images were obtained on a TECNAI G2 F30 transmission electron microscope (acceleration voltage: 300 kV).

4. Electrochemical Measurements

All the electrochemical measurements were carried out with a Bio-Logic VSP electrochemical workstation (Bio-Logic Ni, France). OER performance was measured in a standard three-electrode system using a glassy carbon electrode (GC, 3 mm in diameter, 0.07 cm²) as the supporting working electrode, graphite rod as the counter electrode and mercury/mercury oxide electrode (Hg/HgO) as the reference electrode. Before the electrochemical measurements, 1 M KOH electrolyte was saturated with N₂ for 30 min. To prepare the work electrodes, the catalyst ink was prepared by dispersing 5 mg catalyst and 1 mg carbon black in 1000 μL solution containing 950 μL ethanol and 50 μL 5 wt.% Nafion with sonication for 30 minutes. Then, 5 μL of the acquired slurry was pipetted onto the polished glassy carbon electrode with a surface area of 0.07 cm². The loading of catalysts was about 0.357 mg·cm⁻². All the tests were measured at room temperature (about 25 °C) and the reference electrodes were close to the working electrode through a double salt-bridge and Luggin capillary tip calibrated before and after the electrochemical measurements to make sure the accuracy. The potential was converted by the formula: E(RHE) = E(Hg/HgO) + 0.0591·pH + 0.098 V. The overpotential was calculated by the formula: overpotential (V) = E(RHE) – E(θ), where E(θ) represents the thermodynamic potential for OER (1.23 V vs. RHE). All the potentials used were converted into RHE unless otherwise noted.

Cyclic voltammetry (CV) and Linear sweep voltammograms (LSV). The catalytic performance of samples for OER was evaluated by CV and LSV at a scan rate of 5 mV·s⁻¹ in 1 M KOH solution. All polarization curves were shown with IR-correction by the positive feedback of compensating 80% of the uncompensated solution resistance.

Tafel analysis. The Tafel slope was calculated from the following equation: $\eta = a + b \log(j)$, where η is the overpotential (mV), b is the Tafel slope and j is the current density. It was fitted in the Tafel range.

Electrochemical impedance measurements. The electrochemical impedance spectroscopy (EIS) was recorded in the above three-electrode cell with the frequency varies from 1 MHz to 0.01 Hz in alkaline solution.

ECSA measurements and calculations. The electrochemically active surface area (ECSA) of all catalysts was calculated by the formula: $ECSA = C_{dl}/C_s$, where the double-layer capacitance (C_{dl} in mF) is estimated by plotting the current (i) at various scan rates from 10 to 50 $mV \cdot s^{-1}$ and C_s is the standard specific capacitance ($0.04 mF \cdot cm^{-2}$).^[2] The roughness factor (R_f) was calculated by the formula: $R_f = ECSA/S$, where S is generally equal to the geometric area of the glassy carbon electrode (in this work, $S = 0.07 cm^2$). The applied potential was 0.83–0.93 V vs. RHE in 1 M KOH solution.

Stability test and Chronoamperometry measurements. The dynamic stability was tested by CV at the scan rate of 100 mVs^{-1} for 1000 cycles. After 1000 cycles, the polarization curve was measured under a sweep rate of 5 $mV \cdot s^{-1}$ and compared with its initial curve. Chronoamperometry of OER was tested in 1.48 V vs. RHE for 20 hours.

Specific activity and Turnover frequency (TOF) calculations. The specific activity was obtained by normalizing the apparent current to ECSA. The TOF (s^{-1}) can be calculated with the following equation $TOF (s^{-1}) = I/(4 \cdot F \cdot n)$, where I is the current (A) during linear sweep measurement, F is the Faraday's constant (96485.3 C/mol), n is the number of active sites (mol), factor 4 is based on the consideration that four electrons are required to produce one oxygen molecule.

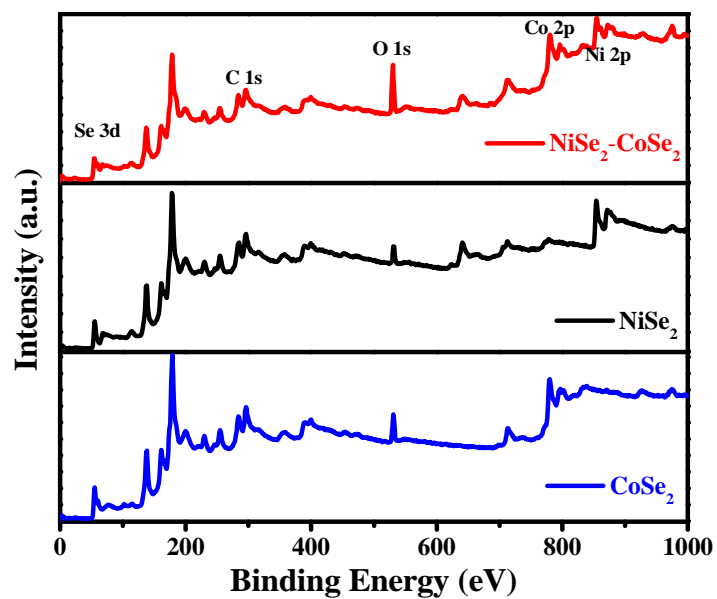


Figure S1. XPS spectrum survey of NiSe₂-CoSe₂, NiSe₂ and CoSe₂.

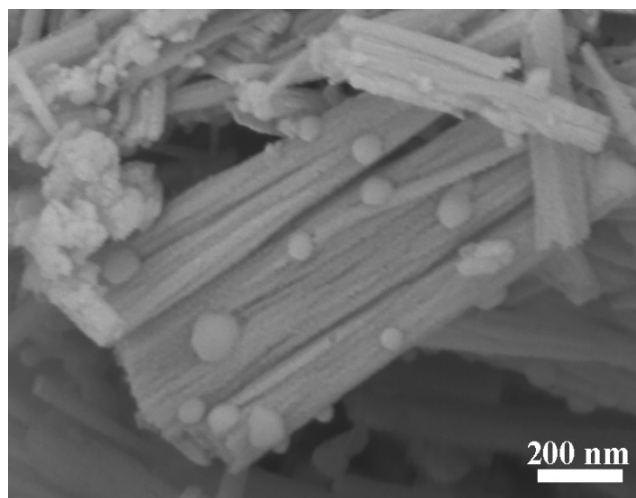


Figure S2a. SEM image of NiCo(OH)_x precursor.

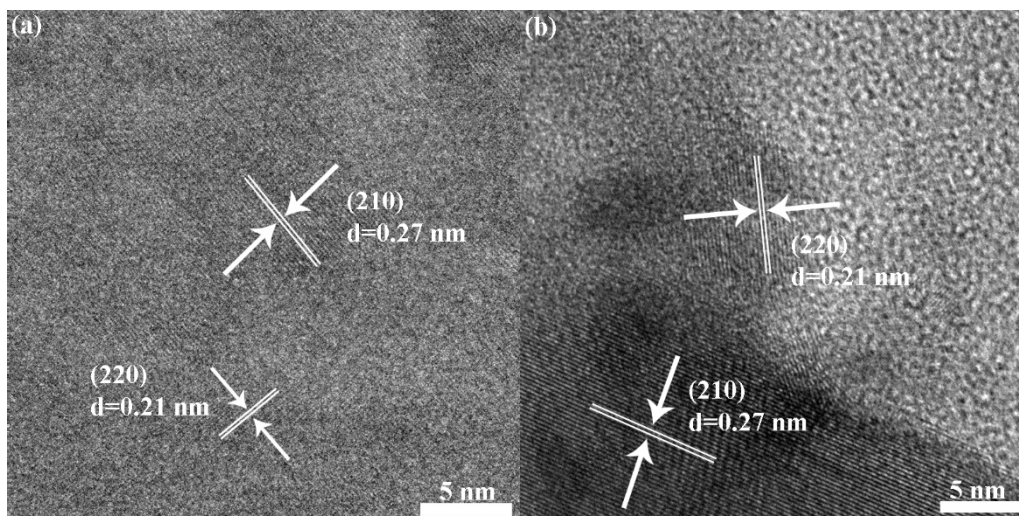


Figure S2b. HR-TEM images of NiSe₂-CoSe₂.

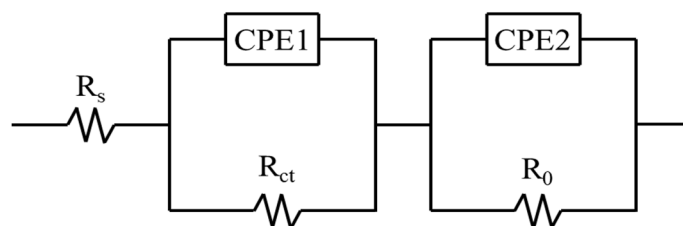


Figure S3. The equivalent circuit used for the Nyquist plot fitting.

In the circuit, R_s is the solution resistance, R_{ct} and R_0 represent interfacial charge transfer resistance and adsorption resistance respectively.

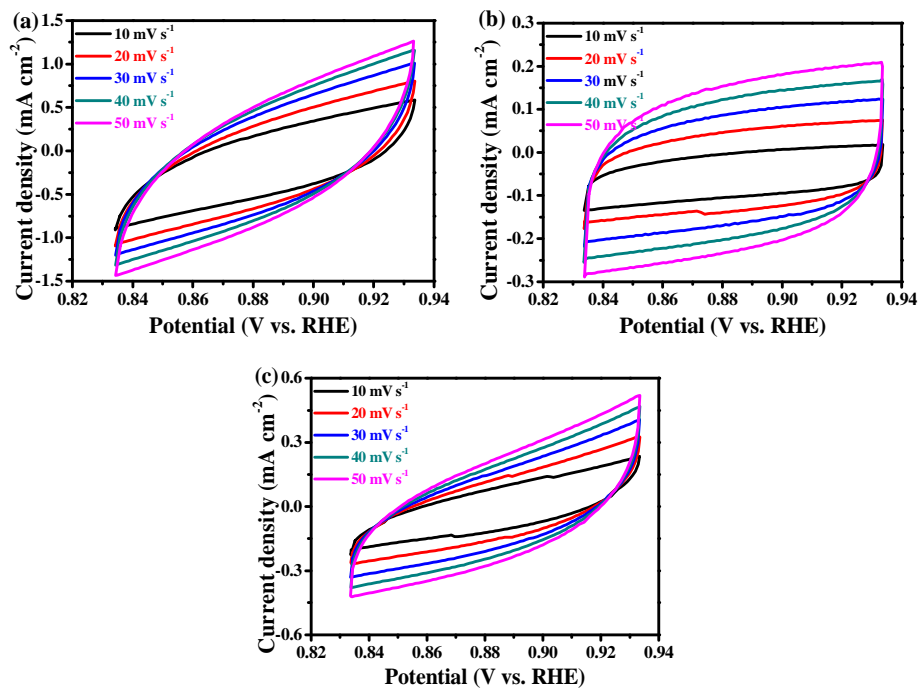


Figure S4. Cyclic voltammograms for the double layer capacitance from 0.834 to 0.934 V vs. RHE of NiSe₂-CoSe₂ (a), NiSe₂ (b), CoSe₂ (c).

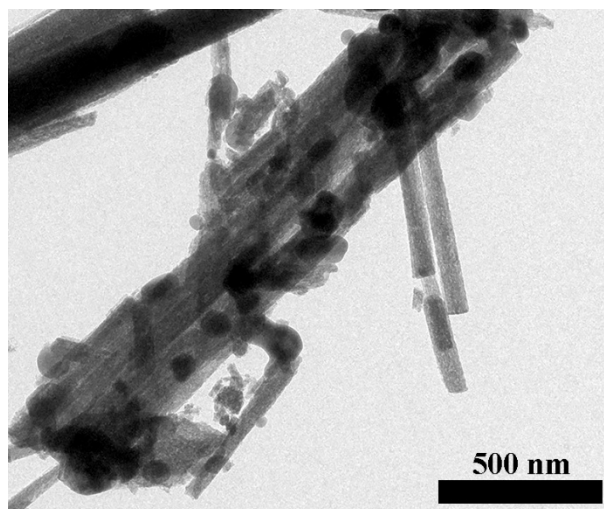


Figure S5. TEM image of NiSe₂-CoSe₂ after the electrochemical stability test.

Table S1. Binding Energy and Relative Content of Ni 2p Obtained from Curve-fitted XPS Spectra for NiSe₂-CoSe₂ and NiSe₂.

Catalysts	Ni 2p _{3/2}		Ni 2p _{1/2}		Relative content
	Peak	Binding energy/eV	Peak	Binding energy/eV	
NiSe ₂ -CoSe ₂	Ni-Se (Ni ²⁺)	853.8	Ni-Se (Ni ²⁺)	871.1	45.0%
	Ni-O (Ni ³⁺)	855.8	Ni-O (Ni ³⁺)	873.8	55.0%
	Sat.	860.8	Sat.	879.5	
NiSe ₂	Ni-Se (Ni ²⁺)	853.1	Ni-Se (Ni ²⁺)	870.4	59.2%
	Ni-O (Ni ³⁺)	855.1	Ni-O (Ni ³⁺)	873.1	40.8%
	Sat.	860.1	Sat.	877.8	

Table S2. Binding Energy and Relative Content of Co 2p Obtained from Curve-fitted XPS Spectra for NiSe₂-CoSe₂ and CoSe₂.

Catalysts	Co 2p _{3/2}		Co 2p _{1/2}		Relative content
	Peak	Binding energy/eV	Peak	Binding energy/eV	
NiSe ₂ -CoSe ₂	Co ⁽⁰⁾	778.2	Co ⁽⁰⁾	793.0	19.3%
	Co ³⁺	780.0	Co ³⁺	795.6	43.4%
	Co ²⁺	781.6	Co ²⁺	797.2	37.3%
	Sat.	785.5	Sat.	802.2	
CoSe ₂	Co ⁽⁰⁾	778.6	Co ⁽⁰⁾	793.4	42.0%
	Co ³⁺	780.4	Co ³⁺	796.0	30.8%
	Co ²⁺	782.0	Co ²⁺	797.6	27.2%
	Sat.	785.9	Sat.	802.6	

Table S3. The Content of Nanoparticles in the NiSe₂-CoSe₂ from EDX Analysis.

Element	Atomic %
Co	9.8
Ni	9.3
Se	52.7
O	28.2

Table S4. The Content of Nanorods in the NiSe₂-CoSe₂ from EDX Analysis.

Element	Atomic %
Co	12.1
Ni	11.3
Se	27.5
O	49.1

Table S5. The Comparison of Ni-based Catalysts in Alkaline Electrolyte for OER.

Materials	Overpotential (mV) @ 10 mA cm ⁻²	Reference
NiSe ₂ -CoSe ₂	250	This work
NiSe ₂ /CoSe ₂ -N	286	[3]
NiSe ₂ /FeSe ₂	256	[4]
CC/CNTs@CoS _{0.74} Se _{0.52}	285	[5]
CoSe ₂ @C-CNT	306	[6]
NiSe ₂ @MoS ₂	267	[7]
P-NiSe ₂ @N-CNTs/NC	306	[8]
Ni _{0.2} Co _{0.8} Se	280	[9]
FeCoMo-Se	264	[10]
(Ni,Co)Se ₂	256	[11]
(Co _{0.21} Ni _{0.25} Cu _{0.54}) ₃ Se ₂	272	[12]
Fe ₃ O ₄ -FeSe/CoSe ₂	279	[13]

Table S6. EIS Fitting Parameters from Equivalent Circuits for Different Catalyst Samples for OER.

Samples	R_s (Ω)	R_{ct} (Ω)	CPE1/S S^{-n}	R_0 (Ω)	CPE2/S S^{-n}
NiSe ₂ -CoSe ₂	6.88	44.4	2.60E-2	12.8	2.66E-3
NiSe ₂	8.09	362.6	3.93E-2	32.7	2.97E-3
CoSe ₂	7.24	284.1	3.45E-2	30.2	3.26E-3

Table S7. The Values of C_{dl} , ECSA and R_f for Different Catalysts.

Samples	C_{dl} (mF·cm ²)	ECSA (cm ²)	R_f
NiSe ₂ -CoSe ₂	8.22	14.39	205.5
NiSe ₂	3.56	6.23	89.0
CoSe ₂	3.57	6.25	89.3

REFERENCES

- (1) Liu, Z.; Zhang, C.; Liu, H.; Feng, L. Efficient synergism of NiSe₂ nanoparticle/NiO nanosheet for energy-relevant water and urea electrocatalysis. *Appl. Catal., B* **2020**, 276, 119165.
- (2) McCrory, C. C. L.; Jung, S.; Peters, J. C.; Jaramillo, T. F. Benchmarking heterogeneous electrocatalysts for the oxygen evolution reaction. *J. Am. Chem. Soc.* **2013**, 135, 16977–16987.
- (3) Zheng, X.; Han, X.; Cao, Y.; Zhang, Y.; Nordlund, D.; Wang, J.; Chou, S.; Liu, H.; Li, L.; Zhong, C.; Deng, Y.; Hu, W. Identifying dense NiSe₂/CoSe₂ heterointerfaces coupled with surface high-valence bimetallic sites for synergistically enhanced oxygen electrocatalysis. *Adv. Mater.* **2020**, 32, 2000607.
- (4) Ni, S.; Qu, H.; Xu, Z.; Zhu, X.; Xing, H.; Wang, L.; Yu, J.; Liu, H.; Chen, C.; Yang, L. Interfacial engineering of the NiSe₂/FeSe₂ p-p heterojunction for promoting oxygen evolution reaction and electrocatalytic urea oxidation. *Appl. Catal., B* **2021**, 299, 120638.
- (5) Zhang, Y.; Qiu, Y.; Ji, X.; Ma, T.; Ma, Z.; Hu, P. A. Direct growth of CNTs@CoS_xSe_{2(1-x)} on carbon cloth for overall water splitting. *ChemSusChem*. **2019**, 12, 3792–3800.
- (6) Yuan, M.; Wang, M.; Lu, P.; Sun, Y.; Dipazir, S.; Zhang, J.; Li, S.; Zhang, G. Tuning carbon nanotube-grafted core-shell-structured cobalt selenide@carbon hybrids for efficient oxygen evolution reaction. *J. Colloid Interface Sci.* **2019**, 533, 503–512.
- (7) Huang, Y.; Huang, J.; Xu, K.; Geng, R. Constructing NiSe₂@MoS₂ nano-heterostructures on a carbon fiber paper for electrocatalytic oxygen evolution. *RSC Adv.* **2021**, 11, 26928–26936.
- (8) Yu, J.; Li, W.; Kao, G.; Xu, C.; Chen, R.; Liu, Q.; Liu, J.; Zhang, H.; Wang, J. In-situ growth of CNTs encapsulating P-doped NiSe₂ nanoparticles on carbon framework as efficient bifunctional electrocatalyst for overall water splitting. *J. Energy Chem.* **2021**, 60, 111–120.
- (9) Qian, Z.; Chen, Y.; Tang, Z.; Liu, Z.; Wang, X.; Tian, Y.; Gao, W. Hollow nanocages of Ni_xCo_{1-x}Se for efficient zinc-air batteries and overall water splitting. *Nanomicro. Lett.* **2019**, 11, 140–156.
- (10) Tang, Y.; Wang, Y.; Zhou, K. In situ oxidation transformation of trimetallic selenide to amorphous FeCo-oxyhydroxide by self-sacrificing MoSe₂ for efficient water oxidation. *J. Mater. Chem. A* **2020**, 8, 7925–7934.
- (11) Song, W.; Teng, X.; Liu, Y.; Wang, J.; Niu, Y.; He, X.; Zhang, C.; Chen, Z. Rational construction of self-supported triangle-like MOF-derived hollow (Ni,Co)Se₂ arrays for electrocatalysis and supercapacitors. *Nanoscale* **2019**, 11, 6401–6409.
- (12) Cao, X.; Johnson, E.; Nath, M. Identifying high-efficiency oxygen evolution electrocatalysts from Co–Ni–Cu based selenides through combinatorial electrodeposition. *J. Mater. Chem. A* **2019**, 7, 9877–9889.
- (13) Zhang, L.; Wang, M.; Chen, H.; Liu, H.; Wang, Y.; Zhang, L.; Hou, G.; Bao, S. Hierarchical growth of vertically standing Fe₃O₄-FeSe/CoSe₂ nano-array for high effective oxygen evolution reaction. *Mater. Res. Bull.* **2020**, 122, 110680.